Center-vortex solutions of the Yang-Mills effective action in three and four dimensions

Dmitri Diakonov
NORDITA, Blegdamsvej 17, 2100 Copenhagen Ø, Denmark
and St. Petersburg Nuclear Physics Institute, Gatchina, St. Petersburg 188 300, Russia

Martin Maul
Department of Theoretical Physics, Lund University, Sölvegatan 14A, S-223 62 Lund, Sweden
(Received 10 April 2002; revised manuscript received 5 August 2002; published 14 November 2002)

We calculate the one-loop effective action of the $SU(2)$ Yang-Mills theory for center-vortex configurations, both in 3D and 4D. We find that in both cases there are minima of the effective action, corresponding to vortices of the transverse size approximately $4/g_3^2$ and $1.7/\Lambda_{\overline{MS}}$, respectively. The values of the effective actions at the minima are *negative*, suggesting that the Euclidian vacuum may be unstable with respect to the creation of vortices.

DOI: 10.1103/PhysRevD.66.096004 PACS number(s): 11.10.Lm, 11.15.Kc, 12.38.−t

I. INTRODUCTION

Recently there have been certain indications from lattice simulations that center-of-group vortices [1,2] may be responsible for the area behavior of large Wilson loops, i.e., for confinement, see, e.g. [3–5] and references therein. If long closed vortices populate the Euclidean vacuum of QCD, resembling curved and entangled spaghetti in Italian *pasta*, it might serve as a microscopic mechanism of confinement.

From the continuum side, however, vortices invoke more questions than there are answers today. First of all, there are no finite-size vortex-type solutions of the classical Yang-Mills (YM) equations in a noncompact space, as the classical equations are dimensionless whereas the functional to be minimized is the transverse energy with the dimension $1/\mathrm{cm}^2$. Therefore, if one finds a solution, its dilatation to larger size will have less energy. This shows that vortex-type solutions of classical equations do not exist [6,7]. In a noncompact space the length scale and hence the vortex radius can only be set by quantum fluctuations. Therefore, vortices can at best arise as saddle points of the effective action, with quantum fluctuations about a trial vortex configuration taken into account. Second, if the effective action contains vortex configurations as saddle points, their energy per unit length in 3D or per unit surface in 4D should be either small positive or, even better, slightly negative. If it is large and positive there is no reason for the vortices to appear in the physical vacuum in the first place. Third, the typical lengths where vortices bend to an angle of the order of unity must be on the average larger than the characteristic transverse size of the vortex. If it is not so, the fluctuation can hardly be called a vortex. Fourth, different vortices in the vacuum or different segments of the same vortex need to be on the average repulsive so that they do not glue up. If vortices are permanently merging and splitting it is difficult to consider them as adequate degrees of freedom. A pilot study of the ''spaghetti vacuum'' in 4D has been performed many years ago by the Copenhagen group [8,9] who considered a 2D lattice of parallel flux tubes and then presented arguments that the lattice should ''melt'' into a disordered phase. Ultimately, one has to build a consistent statistical mechanics of the vortex vacuum in order to see that the ''entangled spaghetti'' has a preferred vacuum free energy as compared to, say, the instanton liquid. The statistical mechanics of instantons is quite a difficult problem by itself [11,12], but vortices are far more difficult to deal with.

In this paper, we address the first and in fact the easiest questions from the above list. For vortices to be physical objects and not artifacts of a regularization and gauge fixing, their typical transverse sizes must be finite in physical units, i.e., to be of the order of $1/g_3^2$ in 3D and of the order of $1/\Lambda_{\mathrm{QCD}}$ in 4D. Correspondingly, the energy of a vortex per unit length should be of the order of g_3^2 in 3D, and the energy per unit surface should be of the order of Λ_{QCD}^2 in 4D. The appearance of Λ_{QCD} implies the transmutation of dimensions through renormalization; it can be achieved only with quantum fluctuations about the vortex taken into due account. We study here the effective action with quantum fluctuations about a trial vortex configuration being integrated out, at the one-loop level. Although the one-loop approximation is not the whole story, it is the first attempt to find out if there are any hints from the continuum Yang-Mills theory that isolated ''thick'' vortices have the right to exist. We seem to get a positive answer to this question. It seems that quantized-flux vortices are dynamically preferred compared with the perturbative vacuum.

In what follows, we consider an idealized isolated infinitely long and straight vortex perpendicular to the (xy) plane. We choose an ansatz for the vortex profile in the transverse plane $\overline{A}_\mu(x,y)$ and expand the YM action into the classical part, $\int d^dx F_{\mu\nu}^2(\overline{A})/4g_d^2$, and the part quadratic in the fluctuations a_μ about the background $\overline{A}_\mu$. Integration over a_μ (and over ghost fields stemming from background gauge fixing) is nontrivial, as the mere counting of levels as compared to the free case is not obvious for the quantized-flux vortices; the difficulty is related to the Aharonov-Bohm effect. We perform this integration by extending the Jost scattering theory (which ''counts'' the levels properly) to the two-dimensional case: it results in the quantum part of the effective action being finite after renormalization. The full effective action is the sum of the classical and quantum parts.

In fact, we study several functional forms of the profile and find that in each case there exists a minimum of the action with respect to the transverse spread of the vortex. It turns out to be about $(4-5)/g_3^2$ in 3D and about $(1.6-1.8)/\Lambda_{\overline{MS}}$ in 4D. The values of the effective action at the minima are *negative* in all cases considered. It indicates that the Yang-Mills vacuum might be unstable in regard to the spontaneous production of vortices.

This work has certain overlap with the earlier study by the Copenhagen group [8,9] who started from the observation by Savvidy [10] that already a constant chromomagnetic field lowers the Yang-Mills vacuum energy. The Savvidy vacuum has, however, a negative fluctuation mode leading to instability. The Copenhagen group has included the amplitude of the negative mode (interpreted as a Higgs field but actually part of the gauge field) into the minimization procedure and indicated that the 2D hexagonal lattice of tubes with quantized flux leads to a further lowering of vacuum energy. However neither the fluctuations in the unstable mode nor in the higher modes were included. In contrast, we take into full account all quantum fluctuations about a *single* trial vortex. The full one-loop quantum calculation performed here shows that already isolated center vortices in $SU(2)$ and also their embedding in $SU(3)$ are energetically preferred compared with the perturbative vacuum. This result comes both in 4D and 3D (the latter case has not been considered in Refs. [8,9]) thus giving certain support to the disordered-vortices scenario of confinement in both cases.

II. THE VORTEX ANSATZ

By definition of a $Z(N)$ vortex, the Wilson loop in the fundamental representation of the $SU(N)$ gauge group, winding around the vortex in the transverse plane assumes values being nontrivial elements of the group center, as the radius of the Wilson loop tends to ∞:

$$\mathrm{P}\exp i\oint A_\mu dx^\mu \to \begin{pmatrix} e^{2\pi ik/N} & & \\ & \cdots & \\ & & e^{2\pi ik/N} \end{pmatrix} \in Z_N, \tag{1}$$

where $k=1,\ldots,N-1$. In this paper, we consider the $SU(2)$ gauge group [although we also make calculations in $SU(3)$ for additional checks]. In $SU(2)$ the only nontrivial element of the center is the minus unity 2×2 matrix. Taking for example a circular Wilson loop of radius ρ in the (xy) plane around a vortex centered at $\rho=\sqrt{x^2+y^2}=0$ we see that only the azimuthal component of the Yang-Mills field is involved in Eq. (1), $A_\phi^a=\epsilon_{\alpha\beta}n_\alpha A_\beta^a$, where n_α is a unit vector in the (xy) plane. One can always choose a gauge where A_ϕ is independent of the azimuthal angle ϕ. Generally speaking, it implies that the radial component A_ρ is nonzero; however, we shall neglect this component as the condition (1) is compatible with $A_\rho=0$. If A_ρ is nonzero it can be reconstructed from gauge invariance by replacing $\partial_\rho\to\partial_\rho\delta^{ab}+f^{acb}A_\rho^c$. A circular Wilson loop in the $J=\frac{1}{2}$ representation lying in the transverse plane and surrounding the vortex center is [13]

$$W_{1/2}(\rho)=\frac{1}{2}\mathrm{Tr}\ \ \mathrm{P}\exp\left(i\oint \rho A_\phi^a t^a d\phi\right)=\cos[\pi\mu(\rho)],$$

$$\mu(\rho)=\rho\sqrt{A_\phi^a(\rho)A_\phi^a(\rho)}. \tag{2}$$

For an arbitrary representation of $SU(2)$, labeled by spin J, one has

$$W_J(\rho)=\frac{1}{2J+1}\frac{\sin[(2J+1)\pi\mu(\rho)]}{\sin[\pi\mu(\rho)]}. \tag{3}$$

If $\mu(\rho)$ tends to an odd integer at large ρ, the Wilson loop $W_J(\rho)\to(-1)^{2J}$. For half-integer representations it is minus unity, hence $\mu(\infty)=2n+1$ is the condition that one deals with a $Z(2)$ vortex. We shall only consider the case when $\mu(\infty)=1$. For simplicity we assume that only one color component of A_ϕ is nonzero:

$$\overline{A}_\phi^a(\rho)=\delta^{a3}\frac{\mu(\rho)}{\rho},\quad \mu(0)=0,\quad \mu(\infty)=1, \tag{4}$$

where $\mu(\rho)$ will be called the profile of the vortex. Equation (4), with all the rest components of the YM field set to zero, is the ansatz for the center vortex field we are going to investigate.

III. THE CLASSICAL ACTION OF THE VORTEX

We take an idealized straight-line (in 3D) or straight-surface (in 4D) vortex whose dimension in the longitudinal direction is $L_\parallel^{(d-2)}$ $(d=3,4)$, while in transverse plane it has a trial profile $\mu(\rho)$. The classical action of the vortex is (see Appendix A)

$$\begin{aligned} S_{\mathrm{class}}&=\frac{1}{4g_d^2}\int d^dx(F_{\mu\nu}^a)^2=\frac{1}{2g_d^2}\int d^{d-2}x_\parallel\int d^2x_\perp(B_\parallel^a)^2\\ &=L_\parallel^{(d-2)}\frac{\pi}{g_d^2}\int_0^\infty d\rho\rho\left[\frac{1}{\rho}\partial_\rho(A_\phi^a\rho)\right]^2\\ &=L_\parallel^{(d-2)}\frac{\pi}{g_d^2}\int_0^\infty d\rho\rho\left[\frac{1}{\rho}\frac{\partial}{\partial\rho}\mu(\rho)\right]^2\equiv L_\parallel^{(d-2)}\mathcal{E}_{\mathrm{class}}. \end{aligned} \tag{5}$$

We remind the reader that in 3D the coupling constant g_3^2 has the dimension of mass, and the theory is convergent. In 4D the (bare) coupling g_4^2 is dimensionless but gets an infinite renormalization from quantum fluctuations. To the one-loop accuracy one can parametrize:

$$\frac{8\pi^2}{g_4^2}=\frac{11}{3}N\ln\frac{M}{\Lambda_{\mathrm{QCD}}}, \tag{6}$$

where M is the ultraviolet cutoff in a particular regularization scheme. The quantum part of the effective action is logarithmically divergent; the renormalizability of the theory ensures that the dependence on the UV cutoff M is canceled in the full effective action.

IV. DIMENSIONAL ANALYSIS

Let us make a quick estimate of the ''best'' transverse size of the vortex ρ_0 from a simple dimensional analysis. We denote the action per unit longitudinal dimension of the vortex by $\mathcal{E}$ such that $S=L_\parallel^{(d-2)}\mathcal{E}$, and call $\mathcal{E}$ the transverse energy of the vortex. If ρ_0 is the scale of the profile function $\mu(\rho)$ [e.g. $\mu(\rho)=\exp(-\rho_0/\rho)$], we find on dimensional grounds that, in 4D

$$\mathcal{E}_{\rm class}=\frac{A}{\rho_0^2}\frac{11N}{24\pi^2}\ln\frac{M}{\Lambda_{\rm QCD}}, \tag{7}$$

where A is the dimensionless functional of the trial profile,

$$A=\pi\rho_0^2\int_0^\infty\frac{d\rho}{\rho}\left(\frac{d\mu}{d\rho}\right)^2. \tag{8}$$

The renormalizability ensures that the quantum part of the effective action has exactly the same coefficient in front of the divergent $\ln M$ piece, but with the opposite sign, so that $\ln M$ cancels in the sum of the classical and quantum parts:

$$\mathcal{E}_{\rm quant}=-\frac{A}{\rho_0^2}\frac{11N}{24\pi^2}\ln(M\rho_0 B),$$

$$\mathcal{E}_{\rm eff}=\mathcal{E}_{\rm class}+\mathcal{E}_{\rm quant}=-\frac{A}{\rho_0^2}\frac{11N}{24\pi^2}\ln(\Lambda_{\rm QCD}\rho_0 B), \tag{9}$$

where A,B are numerical coefficients depending on the concrete functional form of the profile $\mu(\rho)$. $\mathcal{E}_{\rm eff}$ has the minimum at

$$\rho_0^{\rm min}=\frac{\sqrt{e}}{\Lambda B},\quad \mathcal{E}_{\rm eff}^{\rm min}=-\Lambda^2\frac{11N}{24\pi^2}\frac{AB^2}{2e},$$

$$e=2.71828\ldots. \tag{10}$$

In 3D a similar dimensional analysis yields

$$\mathcal{E}_{\rm class}=\frac{A}{g_3^2\rho_0^2},\quad \mathcal{E}_{\rm quant}=-\frac{C}{\rho_0}, \tag{11}$$

with the same coefficient A as in 4D. The sign of C is *a priori* unknown. However, since the theory is superrenormalizable one can suppose that the sign of the quantum energy is the same as in 4D at $M\rho\to\infty$, i.e., negative (direct calculations below confirm the expectation). The sum $\mathcal{E}_{\rm eff}=\mathcal{E}_{\rm class}+\mathcal{E}_{\rm quant}$ then has a minimum at

$$\rho_0^{\rm min}=\frac{1}{g_3^2}\frac{2A}{C},\quad \mathcal{E}_{\rm eff}^{\rm min}=-g_3^2\frac{C^2}{4A}. \tag{12}$$

Notice that both in 3D and 4D we get a natural result for the transverse size of the vortex and a *negative* sign for its transverse energy at the minimum.

In a sense we have already proven the main statements of the paper put in the Abstract and the Introduction: these statements follow from dimensional analysis and the renormalizability of the theory, *provided* the coefficients A,B,C are finite, which is not obvious beforehand. In the rest of the paper we compute these coefficients for different cases, and look for the best profile function $\mu(\rho)$.

V. THE QUANTUM ACTION ABOUT A VORTEX

A. Definition of the quantum action

To get the quantum action for $\mu(\rho)$ we integrate over quantum fluctuations about a given background field $\overline{A}^a_\phi(\rho)$ [see Eq. (4)] considered to be a slowly varying field with momenta $k_\perp$ up to certain $k_{\rm min}$. Accordingly, quantum fluctuations have momenta $k_\perp$ above $k_{\rm min}$ and arbitrary longitudinal momenta. Writing $A_\mu=\overline{A}_\mu+a_\mu$ we expand $F^2_{\mu\nu}(A+a)$ in the fluctuation field a_μ up to the second order appropriate for the 1-loop calculation. The term linear in a_μ vanishes due to the orthogonality of high and low momenta and also because $\overline{A}_\mu$ is in our case independent of ϕ and longitudinal coordinates whereas a_μ is dependent on those coordinates.

The quadratic form for a_μ is the standard (see, e.g. [14])

$$W^{ab}_{\mu\nu}=-[D^2(\overline{A})]^{ab}\delta_{\mu\nu}-2f^{acb}F^c_{\mu\nu}(\overline{A}), \tag{13}$$

if one imposes the background Lorentz gauge condition,

$$D^{ab}_\mu(\overline{A})a^b_\mu=0,\quad D^{ab}_\mu(\overline{A})=\partial_\mu\delta^{ab}+f^{acb}\overline{A}^c_\mu. \tag{14}$$

The quantum part of the effective action is, as usual, given by the small-oscillation determinants:

$$S_{\rm quant}[\overline{A}]=S_{\rm gluon}+S_{\rm ghost}=\frac{1}{2}\ln\det(W^{ab}_{\mu\nu})-\ln\det(-D^2_\mu). \tag{15}$$

Subtraction of free determinants (with zero background field) is understood.

The full effective action is $S_{\rm eff}=S_{\rm class}+S_{\rm gluon}+S_{\rm ghost}$. Since all terms are proportional to the longitudinal dimensions of the vortex $L_\parallel^{(d-2)}$ we shall divide all terms by this quantity; it will then become an equation for the appropriate contributions to the transverse energy of the vortex,

$$\mathcal{E}_{\rm eff}=\mathcal{E}_{\rm class}+\mathcal{E}_{\rm gluon}+\mathcal{E}_{\rm ghost}, \tag{16}$$

where all terms are certain functionals of the trial vortex profile $\mu(\rho)$.

B. The ghost operator

For the vortex ansatz (4) the ghost operator $(D^2)^{ab}$ takes the following simple form in the cylindrical coordinates [13]:

$$D^2=\left(\frac{1}{\rho}\frac{\partial}{\partial\rho}\rho\frac{\partial}{\partial\rho}+\partial_3^2+\cdots\partial_d^2\right)\delta^{ab}+\frac{1}{\rho^2}\left(\delta^{ac}\frac{\partial}{\partial\phi}+f^{a3c}\mu(\rho)\right)\times\left(\delta^{cb}\frac{\partial}{\partial\phi}+f^{c3b}\mu(\rho)\right). \quad (17)$$

The eigenvalues of the structure constants if^{a3c} in the color space are

$$\alpha_c=\begin{cases}\{0,1,-1\} & \text{for } SU(2),\\ \{0,0,1,-1,1/2,1/2,-1/2,-1/2\} & \text{for } SU(3).\end{cases} \quad (18)$$

It is natural to choose a plane wave basis $\exp(ik_\parallel\cdot x_\parallel)$ for the longitudinal directions $x_3,\ldots,x_d$, and a polar basis $\exp(im\phi)Z_m^{(c)}(\rho)$ for the transverse directions. The eigenfunctions $Z_m^{(c)}(\rho)$ satisfy the second-order differential equations depending on the color polarization $c=1,\ldots,(N_c^2-1)$:

$$\left[-\frac{1}{\rho}\frac{\partial}{\partial\rho}\rho\frac{\partial}{\partial\rho}+\frac{(m-\alpha_c\mu(\rho))^2}{\rho^2}\right]Z_m^{(c)}(\rho)=k_{\perp cm}^2Z_m^{(c)}(\rho). \quad (19)$$

For each color polarization c one has to solve a separate eigenvalue equation with a corresponding coefficient α_c from Eq. (18). The spectrum in $k_\perp$ is continuous with the spectral density depending on m and c. By putting the system into a large circular box of radius R, one makes the spectrum discrete, and the eigenvalues $k_\perp$ can be labeled by a discrete number n.

The eigenvalues of the full operator $-D^2$ are then

$$E^2(c,m,n,k_\parallel)=k_\parallel^2+k_{\perp cmn}^2, \quad (20)$$

and one has to sum over the color polarizations labeled by c, the magnetic quantum numbers m, the radial quantum numbers n and integrate over the continuous spectrum in $k_\parallel$. In the free case ($\mu=0$) the eigenfunctions of Eq. (19) are the ordinary Bessel functions $J_{|m|}(k_{0\perp mn}\rho)$ (the index must be nonnegative to ensure the regularity at the origin). In this case the eigenvalues $k_{0\perp mn}$ can be determined by the zeros of the Bessel functions.

According to Eq. (15), the ghost contribution to the transverse energy of the vortex is the sum of logarithms of the eigenvalues:

$$\mathcal{E}_{\rm ghost}=-\sum_{c,m,n,k_\parallel}[\ln E^2(c,m,n,k_\parallel)-\ln E_0^2(c,m,n,k_\parallel)]=-\sum_{c=1}^{N^2-1}\sum_{m=-\infty}^{\infty}\sum_n\int\frac{d^{d-2}k_\parallel}{(2\pi)^{d-2}}\times[\ln(k_\parallel^2+k_{\perp cmn}^2)-\ln(k_\parallel^2+k_{0\perp mn}^2)], \quad (21)$$

where $k_{0\perp\,mn}^2$ are the eigenvalues of the free operator in a box, with $\mu(\rho)$ set to zero. Color polarizations with $\alpha_c=0$ do not contribute since at $\alpha_c=0$ Eq. (19) reduces to the free one.

We first integrate over $k_\parallel$. In the 3D case the integration is finite:

$$\int_{-\infty}^{\infty}\frac{dk_\parallel}{2\pi}\ln\left(\frac{k_\parallel^2+k_\perp^2}{k_\parallel^2+k_{0\perp}^2}\right)=|k_\perp|-|k_{0\perp}|. \quad (22)$$

In the 4D case integration over $k_\parallel$ needs to be regularized. We use the Pauli-Villars regularization scheme, so that henceforth $\Lambda_{\rm QCD}=\Lambda_{P.V.}=e^{1/12}\Lambda_{\overline{MS}}$. We have

$$\int\frac{d^2k_\parallel}{(2\pi)^2}\ln\frac{(k_\parallel^2+k_\perp^2)(k_\parallel^2+k_{0\perp}^2+M^2)}{(k_\parallel^2+k_{0\perp}^2)(k_\parallel^2+k_\perp^2+M^2)}=\frac{1}{4\pi}\left[k_\perp^2\left(\ln\frac{M^2}{k_\perp^2}+1\right)-k_{0\perp}^2\left(\ln\frac{M^2}{k_{0\perp}^2}+1\right)\right]. \quad (23)$$

There is a general formula for summation of any function of eigenvalues becoming continuous in the limit when the box radius goes to infinity; see Sec. VI. In the continuum limit the summation can be replaced by integration over the spectrum with a weight being the phase shift $\delta(k_\perp)$ of the corresponding differential equation, in this case Eq. (19):

$$\sum_n[F(k_n)-F(k_{0n})]=-\frac{1}{\pi}\int_0^\infty dk\,\delta(k)\frac{dF(k)}{dk} \quad (24)$$

(the subscript $\perp$ will be henceforth suppressed). We shall describe the method of finding the phase shifts in Sec. VI. The phase shifts $\delta(k)$ depend on the ''partial wave'' m and on the color polarization c. Let us introduce the accumulated phase shift, summing over all partial waves,

$$\delta_c(k)=2\sum_{m=1}^{\infty}\delta_{cm}(k)+\delta_{c0}(k). \quad (25)$$

Since α_c assumes as many ''plus'' values as there are ''minus'' ones, it is sufficient to sum over nonnegative values of m. [Alternatively, one can take only positive values of α_c but then sum over all m's, positive and negative.] Using the linearity of Eq. (24) in $\delta(k)$ one can introduce the aggregate phase shift of the ghost operator,

$$\delta_{\rm ghost}(k)=\sum_c\delta_c(k). \quad (26)$$

It is a common function both for 3D and 4D. However, the expression for the ghost energy is different in 3D and 4D, as the weights with which eigenvalues are taken are different, cf. Eqs. (22) and (23). Using the general Eq. (24) we obtain the needed transverse energy of the vortex as due to the ghost part of the quantum action:

$$\mathcal{E}^{\rm 3D}_{\rm ghost}=\frac{1}{\pi}\int_0^\infty dk\,\delta_{\rm ghost}(k), \tag{27}$$

$$\mathcal{E}^{\rm 4D}_{\rm ghost}=\frac{1}{\pi^2}\int_0^\infty dk k\,\ln\frac{M}{k}\,\delta_{\rm ghost}(k). \tag{28}$$

C. The gluon operator

We now consider the gluon operator $W^{ab}_{\mu\nu}$; see Eq. (13). Its $(D^2)^{ab}\delta_{\mu\nu}$ part is essentially identical to the ghost operator. For the other part we find the following eigenvalues:

$$\mathrm{Eig}(F^c_{\mu\nu}f^{acb})=\frac{\mu'(\rho)}{\rho}(\{\alpha_c\}_{\rm color}\otimes\{\beta_\lambda\}_{\rm space}),$$

$$\beta_\lambda=\begin{cases}\{0,1,-1\} & \text{for 3D},\\ \{0,0,1,-1\} & \text{for 4D},\end{cases} \tag{29}$$

where the color eigenvalues α_c are the same as for the ghost operator; see Eq. (18).

Therefore, the transverse eigenvalues $k_\perp$ of the gluon operator are found from solving the differential equation for the eigenfunctions $Z^{(c,\lambda)}_m(k_\perp\rho)$ where $c=1,\ldots,(N_c^2-1)$ labels the color polarization and $\lambda=1,\ldots,d$ labels the space polarization of the gluon:

$$\left[-\frac{1}{\rho}\frac{\partial}{\partial\rho}\rho\frac{\partial}{\partial\rho}+\frac{(m-\alpha_c\mu(\rho))^2}{\rho^2}-\frac{2\alpha_c\beta_\lambda\mu'(\rho)}{\rho}\right]Z^{(c,\lambda)}_m(\rho)=k^2_{\perp\,c\lambda m}Z^{(c,\lambda)}_m(\rho). \tag{30}$$

According to Eq. (15), the gluon contribution to the transverse energy of the vortex is the sum of logarithms of the eigenvalues:

$$\mathcal{E}_{\rm gluon}=\frac{1}{2}\sum_{c,\lambda,m,n,k_\parallel}[\ln E^2(c,\lambda,m,n,k_\parallel)-\ln E_0^2(c,\lambda,m,n,k_\parallel)]. \tag{31}$$

Color polarizations with $\alpha_c=0$ cancel from this equation. In 4D there are two space polarizations with $\beta_\lambda=0$ for which the eigenvalue equation (30) reduces to that of the ghost operator, Eq. (19). Therefore, $\mathcal{E}_{\rm ghost}$ is completely canceled by that part of the gluon operator spectrum. In 3D there is only one space polarization with $\beta_\lambda=0$, so that the cancellation is not complete.

Similar to the previous subsection, we introduce the phase shifts $\delta(k)$ but now corresponding to Eq. (30):

$$\delta^{(d)}_{\rm gluon}(k)=\sum_c\sum_\lambda\delta_{c\lambda}(k),$$

$$\delta_{c\lambda}(k)=2\sum_{m=1}^\infty\delta_{c\lambda m}(k)+\delta_{c\lambda 0}(k). \tag{32}$$

Notice that, unlike the ghost case, here the aggregate phase shift depends on the number of dimensions as the number of gluon polarizations λ is d dependent. Using the results of the $k_\parallel$ integration from the previous subsection we can write down the gluon contribution to the transverse energy via the aggregate phase shifts:

$$\mathcal{E}^{\rm 3D}_{\rm gluon}=-\frac{1}{2\pi}\int_0^\infty dk\,\delta^{(3)}_{\rm gluon}(k), \tag{33}$$

$$\mathcal{E}^{\rm 4D}_{\rm gluon}=-\frac{1}{2\pi^2}\int_0^\infty dk k\,\ln\frac{M}{k}\,\delta^{(4)}_{\rm gluon}(k). \tag{34}$$

D. Full quantum energy

Adding up the ghost and gluon contributions to the quantum energy we get

$$\mathcal{E}^{\rm 3D}_{\rm quant}=\frac{1}{\pi}\int_0^\infty dk\left[\delta_{\rm ghost}(k)-\frac{1}{2}\delta^{(3)}_{\rm gluon}(k)\right], \tag{35}$$

$$\mathcal{E}^{\rm 4D}_{\rm quant}=\frac{1}{\pi^2}\int_0^\infty dk k\,\ln\frac{M}{k}\left[\delta_{\rm ghost}(k)-\frac{1}{2}\delta^{(4)}_{\rm gluon}(k)\right]. \tag{36}$$

The combination of ghost and gluon phase shifts in the square brackets will be called the full phase shift; for various cases they are plotted in Figs. 2, 4 and 5.

E. Scaling properties

Let us assume that we have calculated the ghost and gluon phase shifts for a certain profile function $\mu(\rho/\rho_0)$ with $\rho_0=1$ in some arbitrarily chosen units. If we now change ρ_0 all quantities have to scale in accordance with the dimensional analysis of Sec. IV. Equations for $\mathcal{E}^{\rm 3D,4D}_{\rm quant}$ of the previous subsection can be translated into the following expressions for the constants A,B,C introduced in Sec. IV:

$$A=\pi\rho_0^2\int_0^\infty\frac{d\rho}{\rho}(\mu'(\rho))^2, \tag{37}$$

$$C=\frac{\rho_0}{\pi}\int_0^\infty dk\left[\frac{1}{2}\delta^{(3)}_{\rm gluon}(k)-\delta_{\rm ghost}(k)\right], \tag{38}$$

$$\widetilde{A}=\frac{24\rho_0^2}{11N}\int_0^\infty dk k\left[\frac{1}{2}\delta^{(4)}_{\rm gluon}(k)-\delta_{\rm ghost}(k)\right], \tag{39}$$

$$\ln B=-\frac{1}{\widetilde{A}}\frac{24\rho_0^2}{11N}\int_0^\infty dk k\,\ln(k\rho_0)\left[\frac{1}{2}\delta^{(4)}_{\rm gluon}(k)-\delta_{\rm ghost}(k)\right]. \tag{40}$$

As discussed in Sec. IV, the renormalizability of Yang-Mills theory in 4D requires that $\widetilde{A}=A$: if that is satisfied the

TABLE I. Results for flux-0 and flux-1 profiles used. The table shows two columns for each profile: one for $\rho_0=1$ and one for $\rho_0=\sqrt{2}$.

	$\mu(\rho)=\exp(-\rho_0/\rho-\rho/\rho_0)$		$\mu(\rho)=\exp(-(\rho_0/\rho)^3)$		$\mu(\rho)=(\rho/\rho_0)^6/((\rho/\rho_0)^6+1)$	
	$\rho_0=1$	$\rho_0=\sqrt{2}$	$\rho_0=1$	$\rho_0=\sqrt{2}$	$\rho_0=1$	$\rho_0=\sqrt{2}$
A	0.2424	0.2424	2.2333	2.2333	3.3767	3.3767
$N_c=2$:						
$A/\tilde{A}$	1.0603	1.0066	1.0007	0.9862	1.0155	1.0026
B	1.1686	1.0692	1.0388	1.0204	0.8854	0.8923
C	0.1094	0.1089	1.1651	1.1513	1.5025	1.4693
$N_c=3$:						
$\frac{\tilde{A}(N_c=2)}{\tilde{A}(N_c=3)}$	1.0000	0.9999	1.0293	1.0331	1.0107	1.0193
$\frac{B(N_c=2)}{B(N_c=3)}$	1.0082	1.0075	0.8767	0.8750	0.8751	0.8747
$\frac{C(N_c=2)}{C(N_c=3)}$	0.6774	0.6766	0.6484	0.6511	0.6388	0.6387

effective action does not depend on the ultraviolet cutoff M. This relation is, therefore, an important check of the numerics. It can be said that the calculation of $\tilde{A}$ is a particular way of getting numerically the ''11/3'' of the asymptotic freedom law. Further on, we verify the scaling relations (9) and (11) explicitly by changing the scale ρ_0 of the trial functions and checking that $\tilde{A},B,C$ are ρ_0 independent.

Another powerful check of our numerical performance is provided by the number of colors N: the quantities $\tilde{A}$ and B should be independent of N while C must be proportional to N. The calculations successfully pass these tests for the $\tilde{A}$ and C within small errors, whereas the sensitivity of B on the numerics is considerably larger; see Table I.

VI. THE PHASE SHIFT METHOD

The $Z(2)$ vortex field $\mu(\rho)$ with $\mu(0)=0$ and $\mu(\infty)=1$ is very specific from the point of view of differential Eqs. (19) and (30). Near the origin $\rho\approx 0$ the equations resemble the free equation for the Bessel functions $J_m(k\rho)$ while at infinity $\rho\to\infty$ they resemble the equation for $J_{m\pm 1}(k\rho)$, with a shifted index.

This is the essence of quantized $Z(2)$ vortices, see, in this respect, Ref. [13]. This fundamental property of $Z(2)$ vortices causes certain difficulties in finding the continuous spectrum of eigenvalues in a given m sector. We present here an economical method of dealing with this problem; it enables one to find the spectrum unambiguously. We have borrowed the idea of the method from Jost scattering theory, generalizing it to problems with cylindrical symmetry. The application of the phase-shift method to 1-loop calculations of the effective action has been, in general terms, developed in Refs. [15,16].

In the following we consider a general differential equation

$$\left[-\frac{1}{\rho}\frac{\partial}{\partial\rho}\rho\frac{\partial}{\partial\rho}+\frac{m^2}{\rho^2}+U(\rho)\right]Z(\rho)=k^2Z(\rho), \qquad (41)$$

the equation for ghosts (19) and for gluons (30) being exactly of that form.

One looks for the solution which is regular at the origin and follows the oscillatory asymptotics of the Bessel function at infinity:

$$Z(r)=\sqrt{\frac{2}{\pi k\rho}}\cos\left[k\rho-\frac{\pi}{4}-\frac{m\pi}{2}+\delta(k)\right]. \qquad (42)$$

This serves a definition of the phase shift $\delta(k)$. If the system is put in the box of large radius R the zeros of Eq. (42) define the spectrum:

$$k_n=k_{0n}-\frac{\delta(k_n)}{R},\quad k_{0n}=\frac{\pi}{R}\left(n+\frac{3}{4}+\frac{m}{2}\right), \qquad (43)$$

where k_{0n} is the spectrum with zero potential. A sum of any function of the eigenvalues k_n in the continuum limit ($R\to\infty$) becomes

$$\sum_n\left[F(k_n)-F(k_{0n})\right]=-\frac{1}{R}\sum_n F'(k_n)\delta(k_n)$$
$$=-\frac{1}{\pi}\int_0^\infty dk F'(k)\delta(k). \qquad (44)$$

This is Eq. (24) used in the previous section.

In the free case ($U=0$) the differential Eq. (41) has regular solutions $J_m(k\rho)$ (the ordinary Bessel functions), as well as singular solutions $Y_m(k\rho)$ (von Neumann functions). From those one combines Hankel functions,

$$H_m^{\pm}(k\rho)=J_m(k\rho)\pm iY_m(k\rho). \qquad (45)$$

Taking into account that J_m and Y_m are both solutions of the same differential equation, their Wronskian is a constant:

$$W(J_m,Y_m)\equiv k\rho[J_m(k\rho)Y_m'(k\rho)-J_m'(k\rho)Y_m(k\rho)] = \frac{2}{\pi}. \quad (46)$$

Using Eq. (46) one can easily verify that the needed solution $Z_m(k\rho)$ of Eq. (41) satisfies the integral equation:

$$\begin{aligned} Z_m(k\rho) &= J_m(k\rho)-\frac{\pi}{2}\int_0^\rho d\rho'\rho'[J_m(k\rho)Y_m(k\rho') \\ &\quad -J_m(k\rho')Y_m(k\rho)]U(\rho')Z_m(k\rho') \\ &= \mathrm{Im}\left\{ iH_m^{(+)}(k\rho)\left[1-\frac{i\pi}{2}\int_0^\rho d\rho'\rho' H_m^{(-)}(k\rho')\right.\right. \\ &\quad \left.\left.\times U(\rho')Z_m(k\rho')\right]\right\} \\ &= \mathrm{Re}\left\{ H_m^{(+)}(k\rho)\left[1-\frac{i\pi}{2}\int_0^\rho d\rho'\rho' H_m^{(-)}(k\rho')\right.\right. \\ &\quad \left.\left.\times U(\rho')Z_m(k\rho')\right]\right\}. \end{aligned} \quad (47)$$

It enables one to find $Z_m(k\rho)$ iteratively knowing the function at smaller values of ρ, starting from $\rho=0$.

At $\rho\to\infty$ one obtains the asymptotics:

$$\begin{aligned} &A\cos\left[k\rho-\frac{\pi}{4}-\frac{m\pi}{2}+\delta(k)\right] \\ &= \mathrm{Re}\left(e^{i(k\rho-\pi m/2-\pi/4)}\left[1-\frac{i\pi}{2}\int_0^\infty d\rho'\rho' H_m^{(-)}(k\rho')\right.\right. \\ &\quad \left.\left.\times U(\rho')Z_m(k\rho')\right]\right). \end{aligned} \quad (48)$$

Putting $k\rho-m\pi/2-\pi/4=2n\pi$ or $k\rho-m\pi/2-\pi/4=(2n+1/2)\pi$ with n being a large integer and comparing the expressions we obtain the equation for the phase shift:

$$\tan\delta(k)=\frac{\mathrm{Im}\, f_m(k)}{\mathrm{Re}\, f_m(k)},$$

$$f_m(k)=1-\frac{i\pi}{2}\int_0^\infty d\rho\rho H_m^{(-)}(k\rho)U(\rho)Z_m(k\rho). \quad (49)$$

We shall refer to Eq. (49) as the Jost equation as it is closely related to the theory of Jost functions developed in scattering theory; see e.g. [17].

We performed a numerical check of Eq. (49) by taking, as an example, the potential arising from the gluon operator [see Eq. (30)],

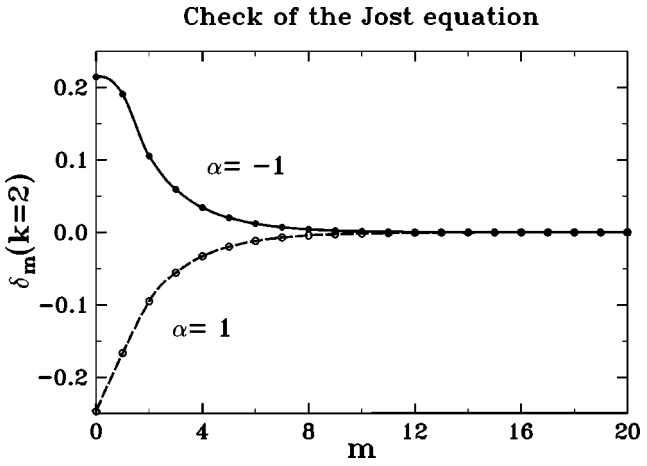

FIG. 1. Check of Eq. (49). For $k=2$, $\alpha=\pm1$ and $\beta=1$ we show the phase shift as a function of m. The solid and dashed lines present the phase shifts as obtained by extrapolating the difference of the zeros, while the open and filled circles show the result as obtained from Eq. (49). One finds perfect agreement between the two methods. It is furthermore seen that the phase shifts decay rapidly in m.

$$U(\rho)=\frac{1}{\rho^2}[(m-\alpha\mu(\rho))^2-m^2-2\alpha\beta\rho\mu'(\rho)], \quad \text{with}\ \ \mu(\rho)=\exp(-\rho-1/\rho). \quad (50)$$

We computed the phase shifts directly from the shift of zeros of $Z_m(k\rho)$ with respect to those of the free $J_m(k\rho)$, and then compared with phase shifts obtained from Eq. (49). The comparison of the two methods is shown in Fig. 1: the agreement is excellent. It is also seen that $\delta_m(k)$ decays fast as a function of m.

One can simplify the method of finding the phase shifts even further. The second integration in Eq. (49) is in fact unnecessary. Indeed, from Eq. (47) one has the identity

$$Z_m(k\rho)=\frac{1}{2}[H_m^{(+)}(k\rho)f_m(k)+H_m^{(-)}(k\rho)f_m^*(k)]. \quad (51)$$

Putting it in the Wronskian [see the definition (46)] we get

$$W(Z_m,H_m^{(-)})=\frac{1}{2}f_m(k)W(H_m^{(+)},H_m^{(-)}) = if_m(k)W(Y_m,J_m)=-\frac{2i}{\pi}f_m(k). \quad (52)$$

Therefore the needed phase shift can be found directly from the Wronskian composed from the solution $Z_m(k\rho)$ and the Hankel function:

$$\delta_m(k)=\mathrm{Arg}(f_m(k))=\mathrm{Arg}\left[\frac{i\pi}{2}W(Z_m,H_{|m|}^{(-)})\right]. \quad (53)$$

Here $\mathrm{Arg}(re^{i\delta})=\delta$ is the argument of a complex number. Notice that Eq. (53) is independent of ρ. Therefore, evaluating the Wronskian in Eq. (52) at different values of ρ is a

valuable check of the stability of the numerics. In fact, this method proves to be quite stable; we actually use it to calculate the phase shifts.

VII. RESULTS

A. Flux-0 vortices

We first consider not a $Z(2)$ but a zero-flux vortex with $\mu(0)=\mu(\infty)=0$. For definiteness we take a smooth profile of the form

$$\mu(\rho)=\exp\left(-\rho-\frac{1}{\rho}\right). \tag{54}$$

Let us briefly describe the numerical procedure. We start by defining a range R for a given value of k and m up to which the differential equations have to be solved. To make sure that we are working in an asymptotic regime we choose $R_{\max}=\max(60.0, x_{|m|15})/k$ where $x_{|m|n}$ is the nth zero of the Bessel function $J_{|m|}(x)$. We have checked that for this choice the phase shifts calculated from Eq. (49) and from Eq. (53) do agree so that we are indeed reaching the asymptotic regime.

The initial condition for finding a regular solution $Z_m(\rho)$ is the free Bessel function which behaves as $J_m(k\rho)\approx(k\rho/2)^m/\Gamma(m+1)$ at small ρ: it is very small at large m. Therefore, for small ρ (actually starting from some finite but small $\rho_{\min}=0.00001/k$ and for $m\geqslant 4$) we solve, instead of Eq. (41), the corresponding equation for the function $B(\rho)=Z(\rho)/((\rho/2)^m/\Gamma(m+1))$,

$$\begin{aligned} B''(\rho)=&-B'(\rho)\frac{2m+1}{\rho} \\ &+\frac{B(\rho)([m-\alpha\mu(\rho)]^2-m^2-2\alpha\beta\rho\mu'(\rho))}{\rho^2} \\ &-k^2B(\rho) \end{aligned} \tag{55}$$

with the initial conditions

$$\begin{aligned} &B(\rho_{\min})=1, \\ &B'(\rho_{\min})=-k\frac{k\rho_{\min}}{2(m+1)}\left(1-\frac{(k\rho_{\min})^2}{4(m+2)}\right). \end{aligned} \tag{56}$$

This differential equation is solved up to the point $R_p=0.9x_{|m|1}/k$ where $x_{|m|1}$ is the first zero of the corresponding Bessel function. Starting from this point the original differential Eq. (41) is solved, with the initial conditions

$$\begin{aligned} Z(R_p)&=\frac{B(R_p)}{\Gamma(m+1)}\left(\frac{kR_p}{2}\right)^m \\ Z'(R_p)&=\frac{B'(R_p)}{\Gamma(m+1)}\left(\frac{kR_p}{2}\right)^m \\ &\quad+\frac{kB(R_p)}{2\Gamma(m)}\left(\frac{kR_p}{2}\right)^{m-1}. \end{aligned}$$

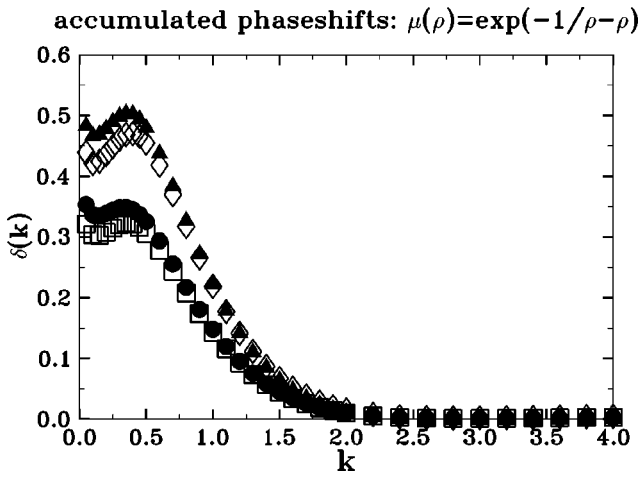

FIG. 2. Full phase shifts $\delta=\frac{1}{2}\delta_{\text{gluon}}-\delta_{\text{ghost}}$ for the profile $\mu(\rho)=\exp(-1/\rho-\rho)$: $\delta^{(3D)}_{N=2}(k)$ (filled circles); $\delta^{(3D)}_{N=3}(k)$ (filled triangles); $\delta^{(4D)}_{N=2}(k)$ (open squares); $\delta^{(4D)}_{N=3}(k)$ (open diamonds).

We have checked that this procedure reproduces the usual Bessel functions in the free case, when $\mu(\rho)=0$.

Having found the regular solution $Z_m(\rho)$, we use it to calculate phase shifts in three different ways. The first method is to use Eq. (49), where the integration goes up to $R_{\max}$. This procedure becomes sometimes unstable because for large ρ the integrand is oscillating. The two other methods exploit Eq. (53). We evaluate the Wronskian either at $0.8R_{\max}$ or at $0.9R_{\max}$. We have checked that except in cases where the phase shift is consistent with zero these three different methods agree with each other. The phase shifts actually used in the results are the ones taken from the Wronskian evaluated at $0.8R_{\max}$.

The individual phase shifts at given k are then accumulated over m, c and λ. Figure 2 shows the total aggregate phase shifts for $N=2,3$ in three and four dimensions. It is seen that in all cases $\delta(k)$ goes to zero quite fast for large k. For very small k values $\delta(k)$ rises again after a maximum at $k=0.4$.

The results are shown in Table I. The A coefficients of the classical and the quantum parts are equal within a small error due to the numerics, as it should be in order to ensure that in four dimensions the results are independent of the UV cutoff M. It is also seen that the A coefficients are independent of the number of colors.

As a final step we check the scaling behavior predicted by Eqs. (9) and (11). To that end we perform the same calculation again but for a profile $\mu(\rho)=\exp(-\sqrt{2}/\rho-\rho/\sqrt{2})$ and compare the result with the one obtained from the profile $\mu(\rho)=\exp(-1/\rho-\rho)$ and assuming the scaling Eqs. (9) and (11). Table I shows indeed that in 3D and 4D the scaling law is satisfied, which is yet another important cross-check of our calculation. Furthermore, it is seen that in all cases we find a minimum of the effective action at negative values, which indicates that the perturbative vacuum is unstable against the production of zero-flux vortices. The values for the minima of the scaling factor are given in Table II. (See also Fig. 3.)

TABLE II. Summary of the physical results with error bars. The physical result is the mean value from the two calculations at $\rho_0 = 1, \sqrt{2}$, while the error is given by the difference of these two values divided by the square root of two.

	$\mu(\rho)=\exp(-\rho_0/\rho-\rho/\rho_0)$	$\mu(\rho)=\exp(-(\rho_0/\rho)^3)$	$\mu(\rho)=(\rho/\rho_0)^6/((\rho/\rho_0)^6+1)$
$N_c=2$:			
$\rho_{0\,\min}^{(3D)}[g_3^{-2}]$	4.441 ± 0.014	3.857 ± 0.032	4.546 ± 0.072
$\mathcal{E}_{\min}^{(3D)}[g_3^2]$	-0.012 ± 0.000	-0.150 ± 0.003	-0.163 ± 0.005
$\rho_{0\,\min}^{(4D)}[\Lambda^{-1}]$	1.477 ± 0.093	1.601 ± 0.020	1.855 ± 0.010
$\mathcal{E}_{\min}^{(4D)}[\Lambda^2]$	-0.005 ± 0.001	-0.040 ± 0.001	-0.046 ± 0.000
$N_c=3$:			
$\rho_{0\,\min}^{(3D)}[g_3^{-2}]$	3.007 ± 0.007	2.506 ± 0.028	2.903 ± 0.046
$\mathcal{E}_{\min}^{(3D)}[g_3^2]$	-0.027 ± 0.000	-0.356 ± 0.008	-0.401 ± 0.013
$\rho_{0\,\min}^{(3D)}[\Lambda^{-1}]$	1.488 ± 0.093	1.403 ± 0.016	1.623 ± 0.009
$\mathcal{E}_{\min}^{(3D)}[\Lambda^2]$	-0.008 ± 0.001	-0.079 ± 0.002	-0.089 ± 0.001

B. Flux-1 vortices

For the calculations with the $Z(2)$ unit-flux vortices we use the following trick which enables us to use the same technique as used for the flux-0 vortices. Instead of the actual flux-1 profile $\mu(\rho)$ with $\mu(0)=0$ and $\mu(\infty)=1$, we consider the profile $1-\mu(\rho)$. From the energy point of view nothing is changed since the classical part depends only on the square of the first derivative of $\mu(\rho)$ while in the quantum part it corresponds to an overall shift of the summation in m. We have checked that in the case of $SU(2)$ this ''reflection'' indeed produces the same results as if one makes the calculation directly with the flux-1 profile $\mu(\rho)$. For the $SU(2)$ vortex embedding into $SU(3)$ this is not the case because here we have a contribution corresponding to the eigenvalues 1/2 in color space and the shift in integer units in the summation over m does not work.

The numerics for the flux-1 vortices is more difficult than for the flux-0 ones. The first problem arises due to the fact that the phase shift exceeds π in magnitude. As the arcus tangent is a multivalued function one then has to reconstruct the true function $\delta(k)$ by adding suitable multiples of 2π so that the resulting function is continuous in k. Furthermore, general constants in terms of suitable multiples of $\pi/4$ have to be added so that the aggregate phase shifts match each other for $k\to\infty$ at a value close to zero.

The second technical problem is that, literally speaking, $\delta(k)$ does not go to zero with $k\to\infty$, but rather approaches a small constant; see Figs. 4 and 5. However, it seems to be a numerical artifact since, as one lowers $\rho_{\min}$ in Eq. (56), the small constant becomes even smaller. Unfortunately, the numerical precision does not allow a complete annihilation of this spurious behavior. In fact, we have to make a cut at the point in k when the function becomes a (tiny) constant. The cross-checks of renormalizability and the N dependence are then satisfied. We obtain, for two different flux-1 profiles,

$$\mu^{(1)}(\rho)=\exp(-1/\rho^3),$$

$$\mu^{(2)}(\rho)=\rho^6/(\rho^6+1), \tag{57}$$

the values of the coefficients in the effective action as given in Table I and Table II. The cross-checks of renormalizability and N dependence are satisfied up to 5% as seen from Table I. Again in all cases the effective action exhibits a minimum. In all cases the minima are at negative values of the effective action, which means that the perturbative YM vacuum is unstable against the production of center vortices in the case of $SU(2)$ in three and four dimensions and that it is even unstable with respect to the production of the embedding of center vortices in $SU(3)$. Comparing the two profiles used it is seen that the powerlike profile $\mu^{(2)}$ gives a slightly deeper minima than the exponential-like profile $\mu^{(1)}$.

VIII. SUMMARY AND OUTLOOK

We have calculated the energy of quantum fluctuations (gluon and ghost) about vortices of various profiles, both in 4 and 3 Euclidean dimensions. Center vortices are peculiar in that the level counting for quantum fluctuations as compared to the free case is not apparent. Because of this, the mere finiteness of the quantum energy in the center-vortex background is not evident before an accurate calculation is performed. We have developed an economical method of ''level counting'' through phase shifts of the appropriate differential operators, which is similar to that used in Jost's scattering theory, and expressed the energy of quantum fluctuations through the phase shifts.

Our results surpass many consistency tests. In 4D we actually manage to calculate numerically and with a good accuracy the ''11/3'' of the asymptotic freedom law; as a result we get the ''transmutation of dimensions'' and express the vortex transverse size and transverse energy in terms of $\Lambda_{\overline{MS}}$; see Table I. The appearance of the ''11/3'' is actually a powerful test of numerical precision. Explicit calculations for different transverse sizes confirm the natural behavior of

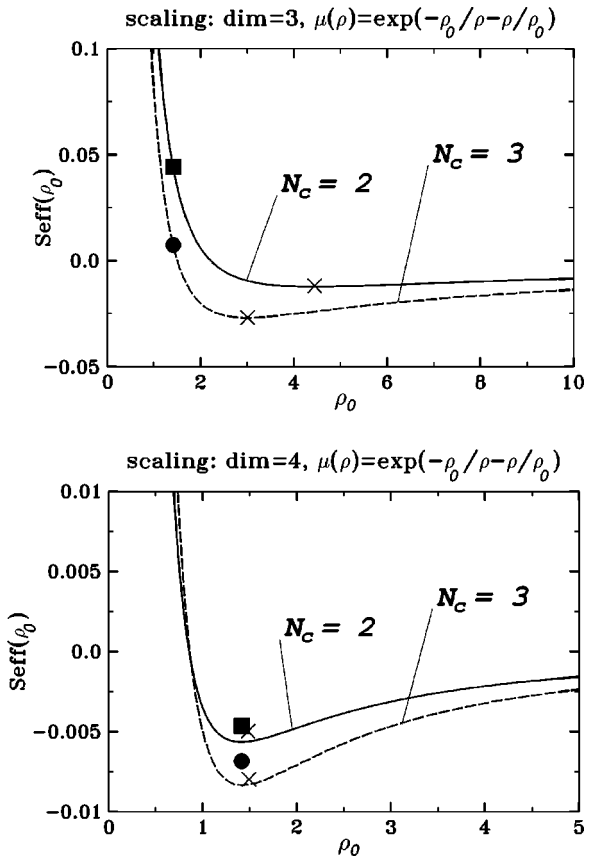

FIG. 3. Scaling behavior of the effective action in three and four dimensions: The figures show the effective action in three and four dimensions for the profile $\mu(\rho)=\exp(-\rho_0/\rho-\rho/\rho_0)$ as a function of ρ_0. The solid line shows the solution for $N_c=2$ and the dashed line for $N_c=3$. The dimensionful constants have been set to 1, i.e., $g_3=1$ in three dimensions and $\Lambda_{\rm QCD}=1$ in four dimensions. The filled circle and the square come from an independent calculation with $\rho_0=\sqrt{2}$ explicitly plugged in. The crosses denote the place of the minimum of the effective action averaged over the results for $\rho_0=1$ and $\rho_0=\sqrt{2}$, cf. Table II.

quantum energy, which follows from dimensions. In addition we verify that the quantum energy is proportional to N_c, as it should be. In our approach, it implies nontrivial sum rules for the phase shifts for gluons and ghosts with different color polarizations.

The effective transverse energy of a vortex (classical plus quantum) has a minimum *lower* than the perturbative vacuum both in 4D and 3D. In 4D this result is in qualitative agreement with the well-known Savvidy's logarithm, $(11N_c/96\pi^2)H^2\ln(H/\Lambda^2\ \text{const})$, for the energy of a constant chromomagnetic field H, following from asymptotic freedom [10]. However, the constant chromomagnetic background has a negative mode [8,9], so that Savvidy's vacuum is unstable. [Because of this negative mode the fluctuation determinant is not well-defined, and the constant in the argument of the logarithm cannot be determined.] In contrast, the vortex has a fast-varying magnetic field, and the fluctuation determinant has no negative mode and can be computed. Qualitatively, the energy gain is expected from dimensional analysis and asymptotic freedom (see Sec. IV) but its value

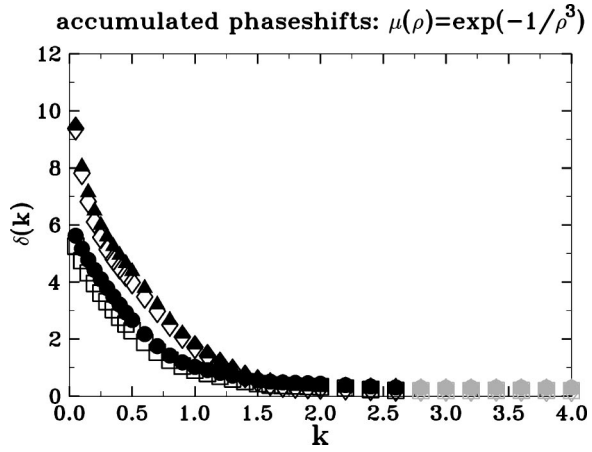

FIG. 4. Full phase shifts $\delta=\frac{1}{2}\delta_{\rm gluon}-\delta_{\rm ghost}$ for the profile $\mu(\rho)=\exp(-1/r^3)$: $\delta^{(3D)}_{N=2}(k)$ (filled circles); $\delta^{(3D)}_{N=3}(k)$ (filled triangles); $\delta^{(4D)}_{N=2}(k)$ (open squares); $\delta^{(4D)}_{N=3}(k)$ (open diamonds). The points in gray have been excluded from the analysis as the function $\delta(k)$ goes over to a spurious constant behavior.

is *a priori* unknown. In 3D one does not have the argument of the asymptotic freedom formula, in favor of the energy gain. Therefore, the fact that we find an energy gain for vortices both in 3D and 4D is nontrivial. The center (flux-1) vortices give a larger energy gain than the nontopological flux-0 ones and from that point of view are dynamically preferred. This was also the conclusion of the Copenhagen group [9] who studied semiclassically a 2D hexagonal lattice made of parallel flux tubes. However, from our calculation we cannot exclude that fluxes of other magnitude, e.g., flux-2 (which are topologically equivalent to flux-0 ones) are even more preferred.

Despite different shapes of vortex profiles considered (one exponential, the other powerlike) we get close numbers for the energy gain. It indicates that vortices are ''soft'' with respect to their deformations in the transverse plane. A further indication in favor of this interpretation is the fast rise of

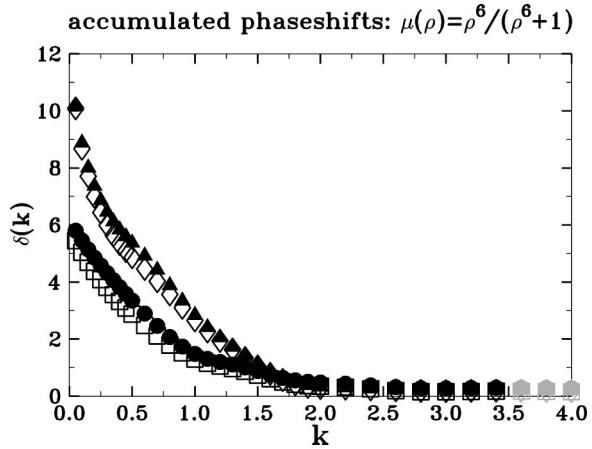

FIG. 5. Full phase shifts $\delta=\frac{1}{2}\delta_{\rm gluon}-\delta_{\rm ghost}$ for the profile $\mu(\rho)=\rho^6/(\rho^6+1)$: $\delta^{(3D)}_{N=2}(k)$ (filled circles); $\delta^{(3D)}_{N=3}(k)$ (filled triangles); $\delta^{(4D)}_{N=2}(k)$ (open squares); $\delta^{(4D)}_{N=3}(k)$ (open diamonds). The points in gray have been excluded from the analysis as the function $\delta(k)$ goes over to a spurious constant behavior.

the aggregate phase at small momenta, see Figs. 2, 4, and 5, although zero modes in a strict sense do not seem to exist; see Appendix B. That makes the search for the absolute minimum in the 1-loop approximation rather problematic: it will be very flat anyhow. Simultaneously, it makes the naive interpretation of thick vortices as neatly shaped spaghetti even more difficult.

Assuming that the vacuum is unstable with respect to the spontaneous production of individual center vortices, their creation can be, in principle, stabilized by (i) kinetic energy of vortex bending, or (ii) repulsive interaction of neighbor vortices and/or of different segments of the same vortex. Concerning vortex interactions, a $Z(N)$ vortex in a regular gauge necessarily has a nonzero azimuthal component of the Yang-Mills field, decaying as $1/\rho$ at large distances from the center in the transverse plane. Two such vortices will then have unacceptable strong repulsion unless they are ''gauge-combed'' in such a way that A_ϕ is zero at large distances. In such a gauge, however, one necessarily gets a Dirac sheet (in 3D) or a Dirac 3-volume (in 4D) of gauge singularities. Dirac singularities from two vortices intersect along a line in 3D or along a surface in 4D. An intersection of two gauge singularities in non-Abelian theory is, generally speaking, not a pure gauge but a physical singularity. It is not clear how to avoid those infinities. In any case, vortex interactions are far from being an easy topic, but they need to be clarified before the statistical mechanics of vortices can tell us that the ''entangled spaghetti'' vacuum has a preferred free energy.

APPENDIX A: CONVERSION INTO CYLINDRICAL COORDINATES

The conversion into cylindrical coordinates is given by the transformations:

$$x=\rho\cos\phi, \quad y=\rho\sin\phi \tag{A1}$$

and

$$\begin{aligned} A_x&=\cos\phi A_\rho-\sin\phi A_\phi,\\ A_y&=\sin\phi A_\rho+\cos\phi A_\phi, \end{aligned} \tag{A2}$$

$$\begin{aligned} \partial_x&=\cos\phi\partial_\rho-\frac{\sin\phi}{\rho}\partial_\phi,\\ \partial_y&=\sin\phi\partial_\rho+\frac{\cos\phi}{\rho}\partial_\phi. \end{aligned} \tag{A3}$$

One finds

$$\begin{aligned} F_{12}&=\partial_x A_y-\partial_y A_x\\ &=\left(\cos\phi\partial_\rho-\frac{\sin\phi}{\rho}\partial_\phi\right)(\sin\phi A_\rho+\cos\phi A_\phi)\\ &\quad-\left(\sin\phi\partial_\rho+\frac{\cos\phi}{\rho}\partial_\phi\right)(\cos\phi A_\rho-\sin\phi A_\phi)\\ &=\frac{A_\phi}{\rho}+\frac{\partial A_\phi}{\partial\rho}, \end{aligned} \tag{A4}$$

using $A_\rho=0$, and with $A_\phi=\mu(\rho)/\rho$ one obtains

$$F_{12}=\mu'(\rho)/\rho \quad\Rightarrow\quad (F_{\mu\nu})^2=2[\mu'(\rho)/\rho]^2. \tag{A5}$$

APPENDIX B: EXCLUDING POSSIBLE BOUND STATES AT $k=0$

The spectrum of the ghost and gluon operators discussed above is incomplete if there exist bound states at $k_\perp=0$. Were the vortices an exact solution of the classical equation of motion, zero modes would be inevitable. However, our vortices are minima of the effective action and not of the classical one, therefore there are no special reasons for zero modes of the small-oscillation operators.

To check whether such states exist we substitute $\rho\to t=1/\rho$ in the gluon operator and obtain the reflected differential equation:

$$-t\frac{\partial}{\partial t}t\frac{\partial}{\partial t}Z(1/t)+\left[(m-\alpha\mu(1/t))^2+2\alpha\beta\frac{\mu'(1/t)}{t}\right]Z(1/t)=0. \tag{B1}$$

α and β are two constants depending on the color and space polarizations of the state under consideration. Using the notation $B(t)=Z(1/t)$ we take the boundary conditions for a bound state $B(0)=0$. This tells only that B has to be regular at the origin. Now we can check the asymptotic of the equation using an explicit flux-1 profile, for example, $\mu(\rho)=\exp(-1/\rho^3)$. One obtains asymptotically for large ρ and correspondingly for small t:

$$\left[-\frac{1}{t}\frac{\partial}{\partial t}t\frac{\partial}{\partial t}+\frac{(m-\alpha)^2}{t^2}\right]B_0(t)=0. \tag{B2}$$

For this equation we require power series in t. The only nontrivial regular solution to this is $B_0(t)=At^{|m-\alpha|}$. Therefore, we use the ansatz

$$B(t)=A(t)t^{|m-\alpha|}. \tag{B3}$$

One obtains the differential equation for the amplitude

$$\left[-\frac{1}{t}\frac{\partial}{\partial t}t\frac{\partial}{\partial t}-2\frac{|m-\alpha|}{t}\frac{\partial}{\partial t}+\frac{(m-\alpha\mu(1/t))^2-(m-\alpha)^2+2\alpha\beta\mu'(1/t)/t}{t^2}\right]A(t)=0. \tag{B4}$$

The boundary conditions are now $A(0)=1$, $A'(0)=0$ to make sure that the asymptotical behavior is correct. Explicit calculation shows that these states behave as

$$Z_m^{(\alpha,\beta)}(\rho) \sim \begin{cases} \rho^{-|m|} & \text{for small } \rho, \ m>0, \\ \rho^{-|m-\alpha|} & \text{for large } \rho, \ m>0. \end{cases} \tag{B5}$$

The behavior at small ρ is clear because of asymptotic arguments like the one used for small t in Eq. (B2). The explicit calculation shows that only irregular solutions exist for $m>0$. In the case $m=0$ the solution is at least logarithmically divergent for large ρ, as $|\alpha|=1,1/2$. Therefore, there are no localized solutions with zero $k_\perp$.

[1] G. 't Hooft, Nucl. Phys. **B138**, 1 (1978).

[2] G. Mack, Cargèse lectures, 1979.

[3] M. Faber, J. Greensite, and S. Olejnik, J. High Energy Phys. **06**, 041 (2000).

[4] L. Del Debbio, M. Faber, J. Greensite, and S. Olejnik, Phys. Rev. D **55**, 2298 (1997).

[5] M. Engelhardt and H. Reinhardt, Nucl. Phys. **B585**, 591 (2000).

[6] The only possible loophole in this analysis, known as ''Derick's theorem,'' is if the field strength of the vortex is allowed to decrease weakly (as $1/\rho$) at large transverse distances. Then the variation of the energy functional with size could have a full-divergence piece which potentially could destroy the argument. [This is what happens in the case of 3D Bogomol'nyi-Prasad-Sommerfield (BPS) monopoles.] Such behavior, however, would lead to the divergent transverse energy. Thus the conclusion that there are no vortex-type solutions of the YM classical equations holds true. In a compactified space the situation is different. In Ref. [7] a vortexlike classical solution has been obtained numerically in a partially compactified $R^2\times T^2$ space with the torus circumference much less than the size of the R^2 box. In this case the scale is set by the compactification circumference. The radius of the vortex has been found to be of the order of the (short) length in the compact direction [7].

[7] A. Gonzalez-Arroyo and A. Montero, Phys. Lett. B **442**, 273 (1998).

[8] H.B. Nielsen and M. Ninomiya, Nucl. Phys. **B156**, 1 (1979); H.B. Nielsen and P. Olesen, *ibid.* **B160**, 380 (1979).

[9] J. Ambjorn and P. Olesen, Nucl. Phys. B: Field Theory Stat. Syst. **B170[FS1]**, 60 (1980); **B170[FS1]**, 265 (1980).

[10] G.K. Savvidy, Phys. Lett. **71B**, 133 (1977).

[11] D. Diakonov and V.Y. Petrov, Nucl. Phys. **B245**, 259 (1984).

[12] D. Diakonov and M. Maul, Nucl. Phys. **B571**, 91 (2000).

[13] D. Diakonov, Mod. Phys. Lett. A **14**, 1725 1909 (1999); **14**, 1909 (1999).

[14] D. Diakonov, V. Petrov, and A. Yung, Phys. Lett. **130B**, 385 (1983).

[15] N. Graham, R.L. Jaffe, M. Quandt, and H. Weigel, Phys. Rev. Lett. **87**, 131601 (2001).

[16] D. Diakonov and V. Petrov, Nucl. Phys. **B306**, 809 (1988); D. Diakonov, V. Petrov, and M. Praszalowicz, *ibid.* **B323**, 53 (1989).

[17] John R. Taylor, *Scattering Theory: The Quantum Theory of Non-Relativistic Collisions* (Wiley, New York, 1972).